

R. G. M. van der Sman
S. van der Graaf

Diffuse interface model of surfactant adsorption onto flat and droplet interfaces

Received: 7 September 2005
Accepted: 20 December 2005
Published online: 23 May 2006
© Springer-Verlag 2006

Paper presented at the Annual European Rheology Conference (AERC) 2005, April 21–23, Grenoble, France.

R. G. M. van der Sman (✉)
S. van der Graaf
Food Process Engineering,
Wageningen University,
Wageningen, The Netherlands
e-mail: ruud.vandersman@wur.nl

Abstract For applications where droplet breakup and surfactant adsorption are strongly coupled, a diffuse interface model is developed. The model is based on a free energy functional, partly adapted from the sharp interface model of [Diamant and Andelman 34(8):575–580, (1996)]. The model is implemented as a 2D Lattice Boltzmann scheme, similar to existing microemulsion models, which are coupled to hydrodynamics. Contrary to these microemulsion models, we can describe realistic adsorption isotherms, such as the Langmuir isotherm. From the free energy, functional analytical expressions of equilibrium properties are derived, which compare reasonably

with numerical results. Interfacial tension lowering scales with the logarithm of the area fraction of the interface unloaded with a surfactant: $\Delta\sigma \sim \ln(1 - \psi_0)$. Furthermore, we show that adsorption kinetics are close to the classical relations of Ward and Tordai. Preliminary simulations of droplets in shear flow show promising results, with surfactants migrating to interfacial regions with highest curvature. We conclude that our diffuse interface model is very promising for apprehending the above-mentioned applications as membrane emulsification.

Keywords Computer modeling · Drop deformation · Emulsion · Surfactant

Introduction

In this paper, we present a diffuse interface model for surfactant adsorption onto the interface of two immiscible fluid, which occurs in emulsions of oil and water. Motivation behind this study is the better understanding of this process, being of significant importance for making emulsions using the novel membranes or microdevices (Sugiura et al. 2004; Schroeder et al. 1998; Abrahamse et al. 2001; Christov et al. 2002; van der Graaf et al. 2004). Despite numerous experimental work (Rayner and Tragardh 2002; Gijsbertsen-Abrahamse et al. 2004), membrane emulsification is still a poorly understood process. Reasons for this is the complex coupling to hydrodynamics, wetting and surfactant dynamics. A more feasible route for understanding is via numerical modelling (Abrahamse et al. 2001; Kobayashi et al. 2004). However, these models only address oil–water systems without

surfactants. Also, from other research fields, there are yet no models capable of addressing adsorption of soluble surfactants onto evolving droplets, which will eventually break off (Pozrikidis 2001; Jacqmin 1999; Li et al. 2000; Wong et al. 1999; Zhou et al. 2002; Eggleton and Stebe 1998; James and Lowengrub 2004).

In this paper, we present a diffuse interface model (Anderson et al. 1998), implemented with Lattice Boltzmann model (see (Chen and Doolen 1998; Swift et al. 1995) for general review), which is in principle, capable of solving the problem of simulating membrane emulsification with surfactants. For describing surfactant adsorption, we have transformed the free energy based, sharp interface model (Diamant and Andelman 1996; Diamant et al. 2001), into a diffuse interface model. There already exist diffuse interface models for microemulsions (Laradji et al. 1992; Theissen and Gompper 1999; Lamura et al. 1999), but they lack a realistic surfactant adsorption isotherm—in contrast

to the model of Diamant and Andelman—which can model the Langmuir and Frumkin adsorption isotherms.

A diffuse interface model has the advantage of being coupled to hydrodynamics (cf. Theissen and Gompper 1999; Lamura et al. 1999). Like the well-known VOF method (Li et al. 2000), a special field tracks the interface without the need of any remeshing of the grid. While the interface is artificially reconstructed in every step of the VOF method, the interface evolves according to chemical potential gradients in the diffuse interface method. The chemical potential is derived from a free energy functional, which includes squared gradient terms for describing the surface free energy in the spirit of van der Waals. Hence, as the diffuse interface method has a firm physical basis (in contrast to VOF), we think it is the most natural method to model surfactant adsorption onto (deforming and breaking) emulsion droplets.

In this paper, we restrict the model to Langmuir adsorption, with equal solubility of the surfactant in both bulk phases. In a subsequent paper, we will introduce the extended model with Frumkin adsorption and differential solubility of the surfactant in the two bulk phases. Furthermore, the current model is two-dimensional (2-D), while we focus on the comparison of analytical prediction and simulations. We first investigate the equilibrium properties of adsorbed surfactants on a planar interface and a circular interface of a droplet. Subsequently, we analyse the dynamics of surfactant adsorption on a planar interface. In conclusion, we briefly investigate the surfactant adsorption on a droplet in linear shear flow, only to indicate the ability of the model to be coupled to hydrodynamics.

Surfactant adsorption model

The emulsion/surfactant system is described with two order parameters, ϕ and ψ , indicating, respectively, the oil/water interface and the surfactant (volume fraction). The system evolves following a convection–diffusion equation, where diffusion of the two order parameters is driven by gradients in the chemical potential (μ_ϕ and μ_ψ). The density ρ and flow field ρu_α is described by the continuity equation and a generalised, incompressible Navier–Stokes equation—which includes a Korteweg–DeVries stress tensor $P_{\alpha\beta}$ representing the effect of interfacial tension on the hydrodynamics. The chemical potential and the Korteweg–DeVries stress tensor are derived from the free energy functional. Below we have listed the governing partial differential equations: (assuming the Einstein convention of summing over double indices):

$$\begin{aligned} \partial_t \phi + \partial_\alpha \phi u_\alpha &= M_\phi \partial_\alpha^2 \mu_\phi \\ \partial_t \psi + \partial_\alpha \psi u_\alpha &= M_\psi \partial_\alpha^2 \mu_\psi \\ \partial_t \rho + \partial_\alpha \rho u_\alpha &= 0 \\ \partial_t \rho u_\alpha + \partial_\beta \rho u_\alpha u_\beta &= -\partial_\beta P_{\alpha\beta} + \partial_\beta \rho \nu (\partial_\alpha u_\beta + \partial_\beta u_\alpha) \end{aligned} \quad (1)$$

with M_ϕ , M_ψ the mobilities of the two order parameters, and ν the kinematic viscosity of the fluid. It is assumed that the bulk phases are incompressible. As discussed below, we implement the model using Lattice Boltzmann, which normally operates in the weakly compressible limit, where the last term in the incompressible Navier–Stokes equation is approximated by $\partial_\beta \nu (\partial_\alpha \rho u_\beta + \partial_\beta \rho u_\alpha)$, which holds true for velocities much smaller than the speed of sound.

Our free energy functional can be decomposed in the following contributions:

$$F = F_{0,\phi} + F_{0,\psi} + F_{ex} + F_1 \quad (2)$$

with

$$\begin{aligned} F_{0,\phi} &= -\frac{A}{2}\phi^2 + \frac{B}{4}\phi^4 + \frac{\kappa}{2}(\partial_\alpha \phi)^2 \\ F_{0,\psi} &= kT[\psi \ln \psi + (1-\psi) \ln(1-\psi)] \\ F_1 &= -\frac{1}{2}\epsilon \psi (\partial_\alpha \phi)^2 \\ F_{ex} &= \frac{1}{2}W\psi\phi^2 \end{aligned} \quad (3)$$

$F_{0,\phi}$ is the common double well free energy functional as used in Cahn–Hilliard theory of an immiscible binary fluid (Anderson et al. 1998). $F_{0,\psi}$ is the entropic part of free energy of mixing of the surfactant with the bulk phase, where we have normalised the surfactant order parameter ψ such that $\psi = 1$ if the interface is fully saturated with surfactant. F_1 is the surface free energy due to surfactant adsorption, F_{ex} is an enthalpic contribution introduced for numerical reasons, as is said to stabilise diffuse interface models of microemulsions (Theissen and Gompper 1999). F_1 is taken from the sharp interface model of Diamant and Andelman of surfactant adsorption, where we have replaced the delta-function, $\delta(x)$, in their (surface) free energy functional with $(\partial_x \phi)^2$. We note that in our numerical simulations we will take the thermal energy as unity, i.e., $kT = 1$, and thus, sets a scale for all other parameters in the free energy functional.

In binary fluid models, the order parameter field, $\phi(x)$, describes a planar interface at $x = 0$ via the profile $\phi(x) = \phi_0 \tanh(x/\zeta)$ (with $\phi_0^2 = A/B$ and $\zeta^2 = 2\kappa/A$). Note that the squared gradient of the profile approximates the delta function.

We obtain the chemical potentials via variational derivatives of the free energy functional (cf. Laradji et al. 1992; Lamura et al. 1999):

$$\begin{aligned} \mu_\phi &= -A\phi + B\phi^3 - \kappa\partial_\alpha^2 \phi + W\psi\phi + \epsilon\psi\partial_\alpha^2 \phi + \epsilon\partial_\alpha \psi \partial_\alpha \phi \\ \mu_\psi &= kT[\ln(\psi) - \ln(1-\psi)] + \frac{1}{2}W\phi^2 - \frac{1}{2}\epsilon(\partial_\alpha \phi)^2 \end{aligned} \quad (4)$$

The Korteweg–deVries pressure tensor is as follows (Theissen and Gompper 1999):

$$P_{\alpha\beta} = p_0 \delta_{\alpha\beta} + q_{\alpha\beta} \quad (5)$$

with p_0 the thermodynamic pressure:

$$p_0 = \phi \mu_\phi + \psi \mu_\psi - F \quad (6)$$

and $q_{\alpha\beta}$ a contribution arising from the Gibbs–Duhem relation:

$$\partial_\alpha P_{\alpha\beta} = (\phi \partial_\alpha \mu_\phi + \psi \partial_\alpha \mu_\psi) \delta_{\alpha\beta} \quad (7)$$

Using the above equation, we find:

$$\begin{aligned} p_0 &= -\frac{1}{2} A \phi^2 + \frac{3}{4} B \phi^4 - \frac{1}{2} \kappa (\partial_\alpha \phi)^2 - \kappa \phi \partial_\alpha^2 \phi \\ &\quad - kT \ln(1 - \psi) + W \psi \phi^2 + \in \phi \partial_\alpha \phi \partial_\alpha \psi + \in \phi \psi \partial_\alpha^2 \phi \\ q_{\alpha\beta} &= (\kappa - \in \psi) (\partial_\alpha \phi) (\partial_\beta \phi) \end{aligned} \quad (8)$$

The diffuse interface model is implemented with a Lattice Boltzmann model, using the D2Q9 model as used in (Swift et al. 1995; Lamura et al. 1999; Theissen and Gompper 1999). The flow field, and the two order parameters are described by three particle distribution functions, f_i , g_i and h_i , from which the following macroscopic fields are derived:

$$\sum_i f_i = \rho; \sum_i c_{i,\alpha} f_i = \rho u_\alpha; \sum_i g_i = \phi; \sum_i h_i = \psi \quad (9)$$

Here, $c_{i,\alpha}$ is the Cartesian component of the particle velocity. These particle distribution functions evolve on a square Bravais lattice, according to a discretisation of the Boltzmann equation, which is given for f_i :

$$f_i(\mathbf{x} + \mathbf{c}_i \Delta t, t + \Delta t) - f_i(\mathbf{x}, t) = -\omega_f [f_i(\mathbf{x}, t) - f_i^{eq}(\mathbf{x}, t)] \quad (10)$$

Here, f_i^{eq} is the equilibrium distribution—which approximates the Maxwell–Boltzmann distribution—of an ideal gas in a simple Lattice Boltzmann (LB) scheme for single-phase fluid dynamics. In the free energy based LB schemes (Swift et al. 1995; Lamura et al. 1999; Theissen and

Gompper 1999), the higher order moments of the equilibrium distribution are related to the chemical potentials and the stress tensor (with the lower order moments linked to the macroscopic fields as defined above):

$$\begin{aligned} \sum_i \tilde{c}_{i,\alpha} g_i^{eq} &= 0 \\ \sum_i \tilde{c}_{i,\alpha} h_i^{eq} &= 0 \\ \sum_i \tilde{c}_{i,\alpha} \tilde{c}_{i,\beta} f_i^{eq} &= P_{\alpha\beta} \\ \sum_i \tilde{c}_{i,\alpha} \tilde{c}_{i,\beta} g_i^{eq} &= \Gamma_\phi \mu_\phi \delta_{\alpha\beta} \\ \sum_i \tilde{c}_{i,\alpha} \tilde{c}_{i,\beta} h_i^{eq} &= \Gamma_\psi \mu_\psi \delta_{\alpha\beta} \end{aligned} \quad (11)$$

with $\tilde{c}_{i,\alpha} = c_{i,\alpha} - u_\alpha$, the so-called peculiar velocity, is a quantity much used in kinetic theory. $\delta_{\alpha\beta}$ is the Kronecker delta. The terms in the chemical potentials and stress tensor which include the gradient and Laplacian of the order parameters are computed with finite difference stencils (cf. Swift et al. 1995).

The transport coefficients are related to the relaxation parameters. The mobilities are equal to:

$$M_\phi = \Gamma_\phi (1/\omega_g - 1/2) \Delta t; M_\psi = \Gamma_\psi (1/\omega_h - 1/2) \Delta t \quad (12)$$

and the kinematic viscosity is equal to:

$$\nu = c_s^2 (1/\omega_f - 1/2) \Delta t \quad (13)$$

Apart for the different form of the free energy functional, our Lattice Boltzmann model is identical as used in Lamura et al. 1999; Theissen and Gompper 1999. Hence, we refer the reader to these papers for more details on the Lattice Boltzmann model.

Equilibrium properties

Analytical results From the above free energy functional we can obtain analytical predictions for the equilibrium properties of surfactant adsorption. In the next paragraph, analytical results are compared with numerical results.

The expression for the adsorption isotherm is obtained by the condition that the chemical potential μ_b of a bulk phase should be equal to the chemical potential at the (planar) interface. Assuming bulk surfactant concentration

(volume fractions), $\psi_b \ll 1$, we have for the chemical potentials of the bulk phases:

$$\mu_{\psi,b} \approx kT \ln \psi_b + \frac{1}{2}W\phi_0^2 \quad (14)$$

Assuming that the sharpness of the diffuse interface is independent of the surfactant loading, the chemical potential at the interface is:

$$\mu_{\psi,0} = kT[\ln(\psi_0) - \ln(1 - \psi_0)] - \frac{1}{2}\in \phi_0^2/\zeta^2 \quad (15)$$

Note that above, we have used $\partial_x \phi(x=0) = \phi_0/\zeta$, as follows from $\phi(x) = \phi_0 \tanh(x/\zeta)$.

In equilibrium $\mu_{\psi,b} = \mu_{\psi,0}$ holds, and after substitution of the above expressions for the chemical potentials, we obtain the Langmuir adsorption isotherm:

$$\begin{aligned} \psi_0 &= \frac{\psi_b}{\psi_b + \psi_c} \\ kT \ln \psi_c &= -\frac{\in \phi_0^2}{2\zeta^2} - \frac{1}{2}W\phi_0^2 \end{aligned} \quad (16)$$

Note that ψ_0 is a dimensionless quantity and attains the value $\psi_0 = 1$ if the surfactant is saturated (if $\psi_b \gg \psi_c$). Further, we note that in the case of $W = 0$, our expressions are equal to those in the model of Diamant and Andelman.

Also, we obtain an analytical expression for the surfactant concentration profile by equating the chemical potential $\mu_\psi(x) = \mu_{\psi,b}$:

$$\psi(x) = \frac{\psi_{b,w}}{\psi_{c,w}(x) + \psi_{b,w}} \quad (17)$$

with

$$kT \ln(\psi_{c,w}(x)) = -\frac{1}{2}\in (\partial_x \phi(x))^2 + \frac{1}{2}W(\phi(x)^2 - \phi_0^2) \quad (18)$$

and $\phi(x) = \phi_0 \tanh(x/\zeta)$.

In sharp interface models, the equation of state is obtained by integration of the Gibbs equation:

$$d\sigma = -\psi_0 d\mu_\psi \quad (19)$$

As we deal with a diffuse interface, the excess amount of surfactant is to be obtained over integration over the diffuse interface (McFadden and Wheeler 2002). Consequently, there exists no analytical expression for the equation of state, but we infer that the excess amount of surfactant is

proportional to ψ_0 , and consequently, that the interfacial tension lowering is proportional to that for a sharp interface: $d\sigma \sim -\psi_0 d\mu_{\psi,0}$. After substitution of Eq. 15 and integration, we obtain the equation of state (cf. Diamant and Andelman (1996)):

$$\sigma(\psi_0) - \sigma_0 \sim kT \ln(1 - \psi_0) \quad (20)$$

$\sigma_0 = 4\kappa\phi_0^2/3\zeta$ is the surface tension of the unloaded droplet.

Numerical analysis We investigate the surfactant concentration profile for a planar interface. First simulations are performed with $\psi_c = 0.017$, $\phi_0 = 10$, $\kappa = \in$, $Ch^* = \zeta/\Delta x = 3$ (grid Cahn number), $Ex = \in/W\zeta^2 \approx 1$, and $\psi_b = \{10^{-4}, 10^{-3}, 10^{-2}\}$. Results are shown in Fig. 1, from which we observe that numerical results are in good agreement with the analytical predictions. In all cases, the order parameter profile, $\phi(x)$, follows the analytical prediction, $\phi(x)/\phi_0 = \tanh(x/\zeta)$, and is thus, independent of surfactant loading as we have assumed above. For low ψ_c and low ψ_b , there is a slight offset in the surfactant concentration at the interface, ψ_0 , probably due to the discretisation error in estimation of the gradients and Laplacian via finite difference stencils. In this case, the gradient of the surfactant concentration at the interface is very sharp ($\psi_0/\psi_b = \mathcal{O}(10^2)$), and a nine-point finite difference stencil for computing gradient and Laplacian terms in chemical potential and stress tensors will not be

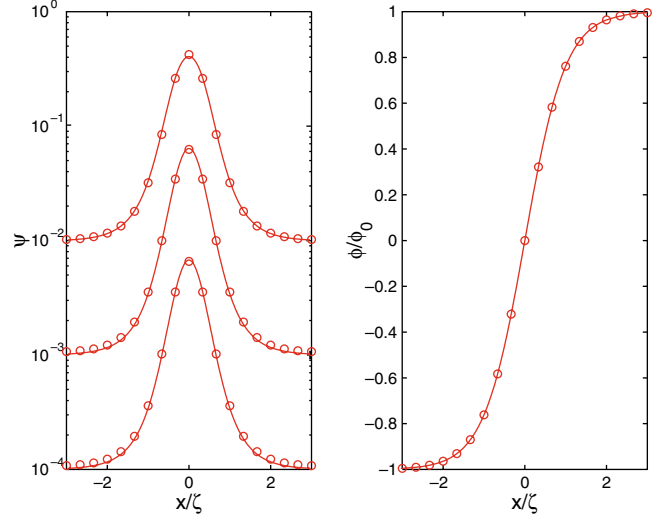


Fig. 1 **a** Profile of the surfactant concentration for a planar interface, located at $x = 0$, for various bulk concentrations $10^{-4} \leq \psi_b \leq 10^{-2}$. Parameter values are listed in the text. Numerical solutions are plotted as symbols, and the solid line is the analytical prediction. **b** Profile of the order parameter, ϕ , according to surfactant adsorption model (symbols) compared to analytical prediction $\phi(x)/\phi_0 = \tanh(x/\zeta)$ (solid line)

very accurate. Better results are expected when using wider stencils, as suggested in other Lattice Boltzmann/Cahn–Hilliard models (Desplat et al. 2001).

Subsequently, we have analysed the validity of the Langmuir adsorption isotherm. $0.002 < \psi_c < 0.08$, $\eta = 0$, $\chi = 0$, $\phi_0 = 10$, $\varepsilon = \kappa$, $Ch^* = 3$, and $Ex \approx 1$. Isotherms resulting from these simulations are shown in Fig. 2. Also shown are the analytical predictions of ψ_0 , using Eq. 16.

One can observe that for high values of ψ_b and ψ_c , the numerical values follow the analytical prediction reasonably well, but at lower levels of ψ_c the predictions are off. This is probably due to discretisation errors in the gradient of ϕ , or violation of the assumption $\psi_b \ll 1$ used above to derive the Langmuir isotherm.

Droplet phase We investigate the lowering of the interfacial tension, $\Delta\sigma$, due to surfactant adsorption on a droplets interface with radius R . At the establishment of equilibrium we have computed $\Delta\sigma = \sigma - \sigma_0$ from σ_0 , the interfacial tension of the bare droplet:

$$\sigma_0 = \frac{4\kappa\phi_0^2}{3\zeta} \quad (21)$$

and the droplets Laplace pressure:

$$\Delta p = \frac{\sigma}{R} \quad (22)$$

Simulations are performed on a 2-D lattice, $L_x/\Delta x = L_y/\Delta y = 64$, and radius, $R = L_x/4$. We have chosen $\kappa = \varepsilon = \zeta = 2$, and different values for ϕ_0 , W , κ , and ψ_b . Initialisation is performed using the above analytical

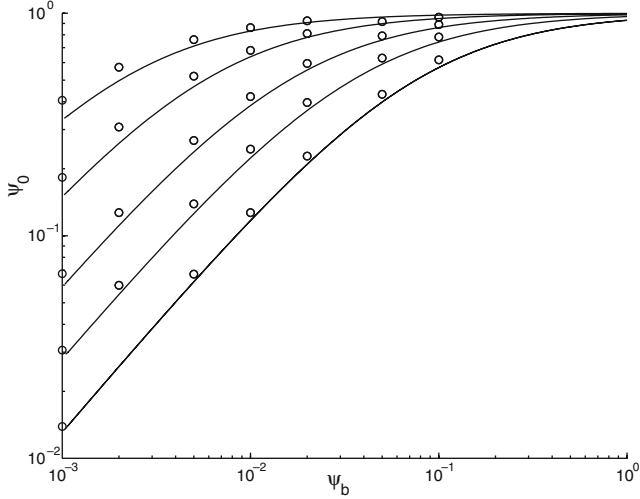


Fig. 2 Adsorption isotherm, showing surfactant loading of a planar interface, ψ_0 , as function of bulk concentration ψ_b for a range of values for $\psi_c = \{0.0020, 0.0056, 0.016, 0.035, 0.075\}$ (from top to bottom). Symbols represent numerical values, and solid lines are analytical predictions

prediction of $\psi(r)$. The density profile is initialised such that the Laplace pressure of the droplet equals that of a droplet with a bare interface. From the resulting surfactant profile at equilibrium, we have determined the surfactant loading of the interface, ψ_0 . In Fig. 3, we have plotted the $\Delta\sigma$ vs $1 - \psi_0$ on a logarithmic scale. The three graphs correspond with the following parameter sets: 1) $\sigma_0 = 6.4$ and $Ex = 1.9$, 2) $\sigma_0 = 14.4$ and $Ex = 0.5$, 3) $\sigma_0 = 24$ and $Ex = 0$. As one can observe for all parameter sets the interfacial lowering, indeed, follows the expected relation $\Delta\sigma \sim \ln(1 - \psi_0)$. However, the scaling clearly depends on Ex , which we, yet, cannot explain theoretically. In the case of $Ex = 0$, we have varied other parameters and have found that interfacial tension lowering only depends on ψ_0 . Observe that for parameter set 1), the relative lowering of the interfacial tension is maximally $\Delta\sigma/\sigma_0 < 0.5$, which is quite a realistic value.

Adsorption dynamics

We have investigated the dynamics of surfactant adsorption for a planar interface, using the classical Ward–Tordai problem (Miller et al. 1994), where one considers an interface in contact with a semi-infinite bulk phase, having initially a homogeneous surfactant concentration, ψ_b , while the interface is depleted of surfactants $\psi_0(t=0) = 0$. Surfactants will diffuse from the bulk phase to the interface. Hence, the surfactant concentration at the interface will rise, while depleting the bulk phase adjacent to the interface, the so-called sublayer. Soon the sublayer will be approximately in equilibrium with the interface, and the increase of the surfactant concentration at the interface will slow down, as the surfactants have to diffuse over longer distances in the

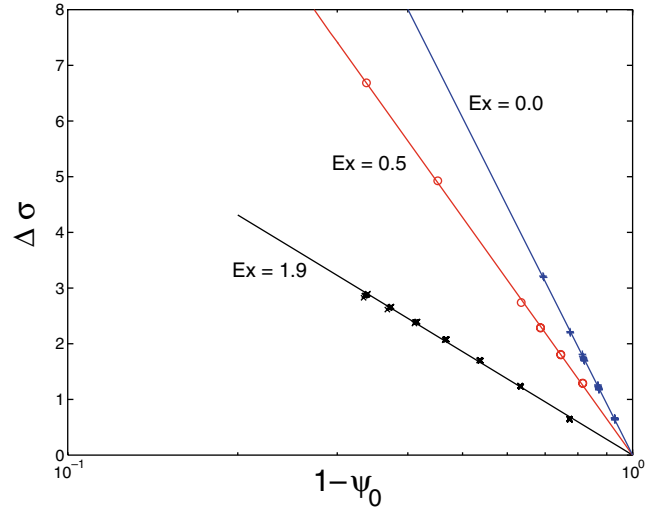


Fig. 3 Interfacial tension lowering $\Delta\sigma$ as function of fraction of non-loaded interfacial area, $1 - \psi_0$. Parameter setting are mentioned in the main text. Numerical results are indicated by symbols, and the solid lines are linear regressions of the numerical data

bulk phase. Such behaviour of the surfactant profile is shown in Fig. 4, which is a result of our numerical analysis of the Ward–Tordai problem. For the Langmuir isotherm the Ward–Tordai can be solved analytically. We will compare our numerical results with approximations of the analytical predictions at short and long time scales.

We have investigated the Ward–Tordai problem, numerically, for a planar interface, in contact with oil and water bulk phases, having equal solubility of the surfactant and equal diffusivity of the surfactant D_ψ . In both bulk phases, we assume Fickian diffusion. As in diffuse interface models, the diffusive mass fluxes are formulated in gradients of the chemical potential ($j_\psi = -M_\psi \nabla \mu_\psi$), the surfactant mobility must be a function of ψ in order to obtain Fickian diffusion (cf. Nauman and He 2001): $M_\psi = D_\psi \psi(1 - \psi)$.

For a diffuse interface model of the Ward–Tordai problem of surfactant adsorption, there exists three-length scales, for which there must be a clear separation of scale. These scales have ζ , the thickness of the diffuse interface, L_ψ , the adsorption length, and L_x , the size of the simulation box. The classical definition of the adsorption length is $L_\psi/\Delta x = \psi_{eq}/\psi_b$ (assuming a sharp interface of thickness Δx). ψ_{eq} follows from the isotherm: $\psi_{eq} = \psi_b/(\psi_b + \psi_c)$. For a diffuse interface model, the adsorption length is a factor two to three larger due to the finite width of the peak in the surfactant profile (see Fig. 4). The (classical) definition of the adsorption length is used to define the reduced time, $\tau = tD_\psi/L_\psi^2$. Simulations are performed with $\zeta \ll L_\psi \ll L_x$ and no-flux boundary conditions at $x = \pm L_x/2$.

As previously stated, we investigate the surfactant adsorption at short and long time scales, for which convenient

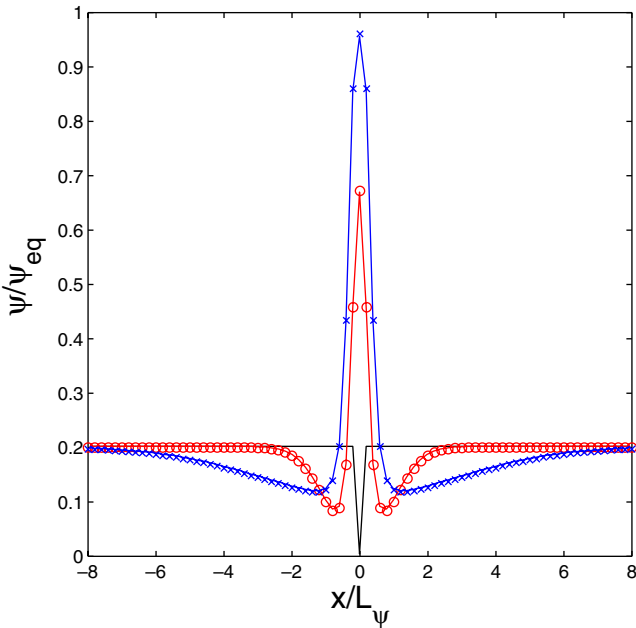


Fig. 4 Surfactant profile, $\psi(x)$, at reduced times, $\tau = 0, 0.5, 2.0$

approximations exists. For a sharp interface, the surfactant adsorption at short times, ($t \rightarrow 0$), in the Ward–Tordai problem follows:

$$\frac{\psi_0(\tau)}{\psi_{eq}} = \frac{2}{\sqrt{\pi}} \sqrt{\tau} \quad (23)$$

The $\sqrt{\tau}$ behaviour holds for arbitrary bulk concentrations and is independent on the type of adsorption isotherm. Due to the finite width of the diffuse interface, we expect the surfactant adsorption in our model to also follow the $\sqrt{\tau}$ behaviour but probably with another proportionality constant. Henceforth, simulations are performed for $\psi_c = 0.0162$, $Ex \approx 0.1$, $\psi_b 10^3 = \{1, 2, 5, 10\}$, $Ch^* = 3$, and $L_x/\Delta x = 400$. Results are shown in Fig. 5, and we view that all sorption curves, $\psi(\tau)/\psi_{eq}$, for different ψ_b collapse to a single curve for short times at $\tau < 0.02$:

$$\frac{\psi_0(\tau)}{\psi_{eq}} \approx \frac{5}{\sqrt{\pi}} \sqrt{\tau} \quad (24)$$

This means that the adsorption length in the adsorption length for a diffuse interface is 0.4 times smaller than the adsorption length as defined for a sharp interface.

Surfactant adsorption at long times is shown in Fig. 6. Simulations are performed with same parameter set as above; only the bulk concentrations are in the range of $\psi_b = \{0.05, 0.1, 0.2\}$, giving a small adsorption length in the order of $L_\psi \approx 20$ and Langmuir number of $La = \psi_b/\psi_c \approx \{3, 6, 12\}$. At long times, the surfactant loading of the interface can be approximated (cf. Mysels (1985)):

$$\frac{\psi_0}{\psi_{eq}} = 1 - \frac{1}{\sqrt{(\pi\tau)} - La(1 - \sqrt{(\pi\tau)})} \quad (25)$$

These approximations are drawn in Fig. 6 as dashed lines, and follow reasonably close to our numerical results.

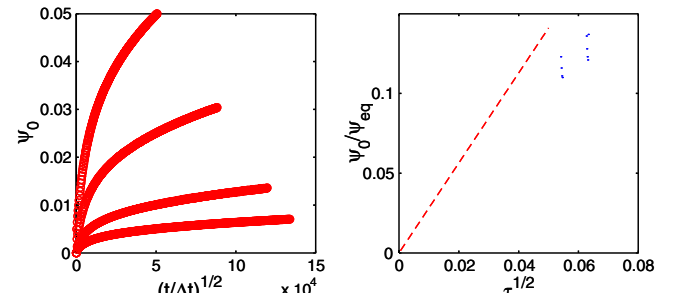


Fig. 5 Evolution of surfactant loading of the interface at short time scale, a in real time t and b in reduced time τ . Dashed line shows the limiting behaviour at $\tau \rightarrow 0$. Values of ψ_b are listed in the text

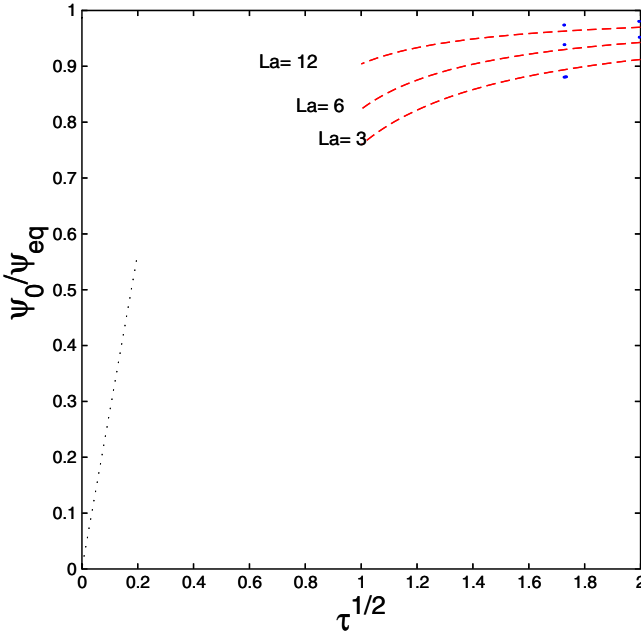


Fig. 6 Evolution of surfactant loading of the interface in reduced time for Langmuir numbers, $\text{La} = \psi_b/\psi_c \approx 3, 6, 12$. The *Dashed line* shows the limiting behaviour at $\tau \rightarrow \infty$, and the *dotted line*, the short time behaviour. Values of ψ_b are listed in the text

At long times, the adsorption is determined by the diffusion from distances $l \ll L_\psi$ to the subsurface layer, and therefore, the finite width of the diffuse interface, ζ , does not play a role in the adsorption kinetics. At short times, we have found that the finite size of the diffuse interface does affect the kinetics, leading to an apparent adsorption length of $L' = 0.4L_\psi$. The apparent adsorption length depends on ζ and also the initial surfactant loading of the interface at $t = 0$. For our simulations, we have chosen to set $\psi(x) = 0$ for $x = 0$ and $\psi(x) = \psi_b$ for $x \neq 0$. An alternative initial condition is $\psi(x) = 0$ for $|x| < 2\zeta$, which probably will lead to a larger apparent adsorption length.

Surfactant adsorption on evolving droplets

To demonstrate that our diffuse interface model of surfactant adsorption can be coupled to hydrodynamics, we have performed preliminary simulations of a surfactant-laden drop in a uniform flow field and a linear shear field. By simulating the drop in a uniform flow field, we investigate the Galilean invariance of a droplet in equilibrium, the bulk phases having a surfactant bulk concentration of ψ_b . By simulation of a deforming droplet, we investigate whether the surfactant will diffuse over the interface of a deforming droplet.

Simulations are performed on a lattice of $L_x = 96\Delta x$ by $L_y = 48\Delta x$ lattice cells, with constant velocity boundary conditions at the top and bottom wall and periodic boundary conditions at the side walls. The droplet has a radius of

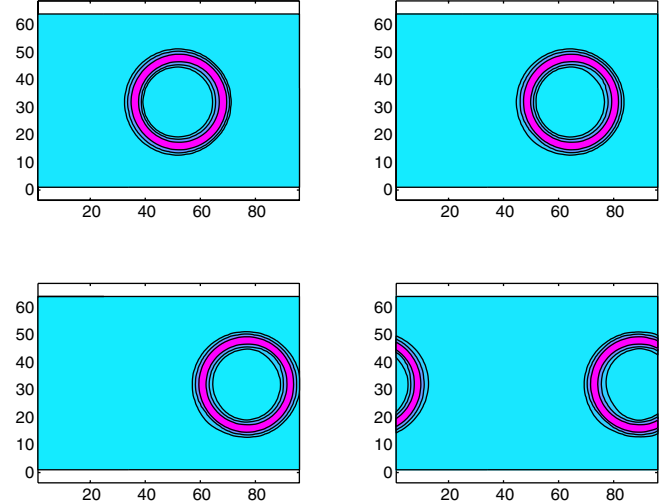


Fig. 7 Contour plot of surfactant concentration of a surfactant-laden droplet translating in a uniform flow field

$R = 12\Delta x$, and is initially in equilibrium with the bulk phase. Furthermore, the Courant number is $Cr = u_{\text{wall}}\Delta t/\Delta x = 0.005$, the Peclet number is $Pe = u_{\text{wall}}R/D_\psi = 533$, $\psi_c = 0.016$, $\text{La} \approx 1$, the Reynolds number is $Re = 0.3$.

Snapshots of the translating droplet in a uniform flow field are shown in Fig. 7. Here, the contour plot of the surfactant concentration is depicted. The maximum surfactant concentration coincides with the droplet interface and follows that the droplet is translating in the flow field. However, if the Peclet number becomes a magnitude higher, the surfactant is not able to follow the motion of the droplet and shows unphysical aggregation at the poles of the droplet.

By reversing the velocity of the top plate, we simulate the droplet in a shear field. Simulation is performed for a capillary number of $Ca = \gamma R \mu / \sigma_0 = 0.1$ with $\gamma = 2u_{\text{wall}}/L_y$,

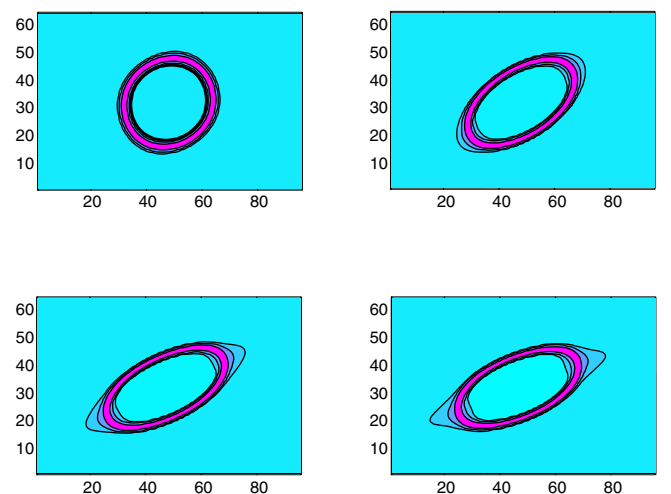


Fig. 8 Contour plot of surfactant concentration of a surfactant-laden droplet deforming in linear shear field

the shear rate, μ , the dynamic viscosity of continuous phase, and σ_0 , the interfacial tension of a bare interface.

Snapshots of the droplet in shear flow are shown in Fig. 8. Observe that at the poles, the surfactant has migrated slightly from the poles to the regions with highest curvature, as one should expect (Pozrikidis 2001; Stone 1994). We have found that stability of the scheme is subtle and needs more careful investigation of the wide set of numerical parameters in the model.

Conclusions

We have developed a diffuse interface model for surfactant adsorption onto the interface of an evolving droplet. In contrast to diffuse interface models of microemulsions, our model exhibits realistic adsorption isotherms named the Langmuir isotherm.

For the equilibrium, we have derived analytical expressions, which are in reasonable agreement with our numerical results. Differences arise due to discretisation errors in the finite difference approximations of the gradients and Laplacian of the order parameters, ϕ and ψ . We expect accuracy to improve if wider stencils are used for these finite differences (cf. Desplat et al. (2001)). Lowering of interfacial tension, σ , of a droplet due to surfactant adsorption, follows the correct theoretical behaviour of $\Delta\sigma \sim \ln(1 - \psi_0)$.

The dynamics of surfactant adsorption of the diffuse interface model simulating the classical Ward–Tordai problem is very similar to the dynamics of a sharp interface model. At short times, we have found that the surfactant loading follows $\sqrt{(\tau)}$ behaviour. However, correct initial conditions are to be used to obtain the same proportionality factor. At long times, the surfactant adsorption does follow

quite closely the approximation, which holds for sharp interface models.

Via brief simulations of a surfactant-laden drop in a (shear) flow field, we have shown that our diffuse interface model can be coupled to hydrodynamics. Upon deformation of the droplet, the surfactants diffuse to the part of the droplet interface with the highest curvature.

We view that our model holds great potential in addressing problems, where hydrodynamics and surfactant adsorption are strongly coupled (e.g., membrane emulsification), and especially problems involving droplet break-up—which is modelled with much ease in diffuse interface models (Jacqmin 1999). Our model can also provide a sound physical description for the complex rheology of surfactant-stabilized emulsions or compatibilized polymer blends, which is governed by continuous droplet/domain deformation, or even breakup and coalescence (van Puyvelde et al. 2001; Blawzdziewicz et al. 2000). Our model lifts the restriction to insoluble surfactants of existing volume-of-fluid models (cf. Blawzdziewicz et al. (2000)). Hence, our model can impart a *major* step forward in numerical modeling of the rheology of these complex fluids.

Bear in mind that our model is yet limited to 2-D, non-ionic surfactants, with bulk concentrations below the critical micelle concentration (CMC). Extension to 3-D is straightforward for diffuse interface Lattice Boltzmann models (Desplat et al. 2001). The other extensions do not present a problem in principle, as ideas for studies as in Diamant and Andelman 1996; Liao et al. 2003, can also be implemented with ease.

Acknowledgements We thank Gerhard Gompper and Reinhardt Miller for the fruitful discussions.

References

- Abrahams AJ, van der Padt A, Boom RM, de Heij WBC (2001) Process fundamentals of membrane emulsification: simulation with CFD. *AIChE J* 47 (6):1285–1291
- Anderson DM, McFadden GB, Wheeler AA (1998) Diffuse interface methods in fluid mechanics. *Annu Rev Fluid Mech* 30:139–165
- Blawzdziewicz J, Vlahovska P, Loewenberg M (2000) Rheology of a dilute emulsion of surfactant-covered spherical drops. *Physica A* 276(1–2):50–85
- Chen S, Doolen GD (1998) Lattice Boltzmann method for fluid flows. *Annu Rev Fluid Mech* 30:329–364
- Christov NC, Ganchev DN, Vassileva ND, Denkov ND, Danov KD, Krachevsky PA (2002) Capillary mechanisms in membrane emulsification: oil-in-water emulsions stabilized by Tween 20 and milk proteins. *Colloids Surf A* 209:83–104
- Desplat JC, Pagonabarraga I, Bladon P (2001) LUDWIG: a parallel Lattice–Boltzmann code for complex fluids. *Comput Phys Commun* 134(3):273–290
- Diamant H, Andelman D (1996) Kinetics of surfactant adsorption at fluid/fluid interfaces: non-ionic surfactants. *Europhys Lett* 34(8):575–580
- Diamant H, Ariel G, Andelman D (2001) Kinetics of surfactant adsorption: the free energy approach. *Colloids Surf A* 183–185:259–276
- Eggleton CD, Stebe K (1998) An adsorption–desorption-controlled surfactant on a deforming droplet. *J Colloid Interface Sci* 208:68–80
- Gijsbertsen-Abrahams AJ, van der Padt A, Boom RM (2004) Status of cross-flow membrane emulsification and outlook for industrial application. *J Membr Sci* 230(1–2):149–159
- Graaf S. van der, Schroen CGPH, van der Sman RGM, Boom RM (2004) Influence of dynamic interfacial tension on droplet formation during membrane emulsification. *J Colloid Interface Sci* 277(2):456–463

- Jacqmin D (1999) Computation of two-phase Navier–Stokes flows using phase field modeling. *J Comput Phys* 155:96–127
- James AJ, Lowengrub J (2004) A surfactant conserving volume-of-fluid method for interfacial flows with insoluble surfactant. *J Comput Phys* 201(2):685–722
- Janssen J JM, Boon A, Agterof WGM (1994) Influence of dynamic interfacial properties on droplet breakup in simple shear-flow. *AIChE J* 40(12):1929–1939
- Joos P, van Uffelen M (1995) Theory on the growing drop technique for measuring dynamic interfacial tensions. *J Colloid Interface Sci* 171:297–305
- Kobayashi I, Mukataka S, Nakajima M (2004) CFD simulation and analysis of emulsion droplet formation from straight-through microchannels. *Langmuir* 20:9868–9877
- Lamura A, Gonella G, Yeomans JM (1999) A lattice Boltzmann model of ternary fluid mixtures. *Europhys Lett* 45 (3):314–320
- Laradji M, Guo H, Grant M, Zuckermann MJ (1992) The effect of surfactants on the dynamics of phase separation. *J Phys: Condensed Matter* 4:6715–6728
- Li J, Renardy Y, Renardy M (2000) Numerical simulation of breakup of a viscous drop in simple shear flow through a volume-of-fluid method. *Phys Fluids* 12:269
- Liao YC, Basaran OA, Franses EJ (2003) Micellar dissolution and diffusion effects on adsorption dynamics of surfactants. *AIChE J* 49(12):3229–3240
- McFadden GB, Wheeler AA (2002) On the Gibbs adsorption equation and diffuse interface models. *Proc R Soc Lond A* 458:1129–1149
- Miller R, Joos P, Fainerman VB (1994) Dynamic surface and interfacial tensions of surfactant and polymer solutions. *Adv Colloid Interface Sci* 49:249–302
- Mysels KJ (1985) Diffusion controlled adsorption on a plane: non-ideal isotherms. *Colloids Surf* 16:21–29
- Nauman EB and He DQ (2001) Non-linear diffusion and phase separation. *Chem Eng Sci* 56:1999–2018
- Pozrikidis C (2001) Interfacial dynamics for Stokes flow. *J Comput Phys* 169: 250–301
- Puyvelde P van, Velankar S, Moldenaers P (2001) Rheology and morphology of compatibilized polymer blends. *Curr Opin Colloid Interface Sci* 6(5–6): 457–463
- Rayner M, Tragardh G (2002) Membrane emulsification modeling: how can we get from characterisation to design? *Desalination* 145(1–3):165–172
- Schroeder V, Behrend O, Schubert H (1998) Effect of dynamic interfacial tension on the emulsification process using microporous, ceramic Membranes. *J Colloid Interface Sci* 202:334–340
- Stone HA (1994) Dynamics of drop deformation and breakup in viscous fluids. *Annu Rev Fluid Mech* 26:65–102
- Sugiura S, Nakajima M, Oda T, Satake M, Seki M (2004) Effect of interfacial tension on the dynamic behavior of droplet formation during microchannel emulsification. *J Colloid Interface Sci* 269:178–185
- Swift MR, Orlandini E, Osborn WR, Yeomans JM (1995) Lattice Boltzmann simulations of liquid–gas and binary fluid mixtures. *Phys Rev E* 54(5):5041–5052
- Theissen O, Gompper G (1999) Lattice Boltzmann study of spontaneous emulsification. *Eur Phys J B* 11:91–106
- Wong H, Rumschitzki D, Maldarelli C (1999) Marangoni effects on the motion of an expanding or contracting bubble pinned at a submerged tube tip. *J Fluid Mech* 379:279–302
- Zhou H, Cristini V, Lowengrub J, Macosko CW (2002) Numerical simulation of drop breakup and coalescence with soluble surfactant in 3D. 74th Annual Meeting Soc Rheology